

## Pipe resonance: A novel approach to measuring local speed of sound

Emily Lau  
*PHYS 229*

Research Partner: Alasdair Buchanan

The local speed of sound is a variable that is important to know for various science and engineering applications, such as acoustic design, ultrasound imaging, and sonar. This experiment aimed to explore the accuracy of using pipe resonance and mathematical model fitting to find the local speed of sound in comparison to literature values. A Bluetooth speaker was set up to play white noise (all-frequency noise with even frequency distribution) through an open-open pipe containing a microphone connected to an oscilloscope taking time-domain data. This data was then fast Fourier transformed and fitted to a mathematical model to retrieve the local speed of sound and the end correction coefficient. This fit yielded a value of  $337.5 \pm 13.81$  m/s for the speed of sound, which matched the expected value of 343.7 m/s within uncertainty. Although future experiments would be required to increase precision, the utilization of pipe resonance and analytical fit methods is a promising avenue of determining the local speed of sound.

## I. INTRODUCTION

The speed of sound is a local variable that is important to know for various purposes, including sonar and ultrasonic sensor tools. Therefore, it can be helpful to explore different methods for determining the local speed of sound, such as the use of fitting a mathematical model to the resonance frequency data of white noise (all-frequency noise with even frequency distribution) through a pipe.

The resonance frequency of an object is the frequency at which the object will naturally oscillate maximally with minimal effort. In the case of an open-open pipe, it is the frequency at which the anti-nodes of the standing wave within the pipe will occur at a maximal amplitude. It is determined by the formula  $f = \frac{nv}{2(L+kR)}$ , where  $n$  is a number corresponding to the number of wavelengths within the pipe,  $v$  is the speed of sound,  $L$  is the length of the pipe,  $k$  is the end correction coefficient, and  $R$  is the radius of the pipe. This formula is a well-known formula for the resonance frequency of open-open pipes [1], with the addition of a term accounting for end correction; end correction is a phenomenon of open-open pipes where the nodes are actually not exactly at the ends of the pipes, but instead a little past the ends.

A Bluetooth speaker was used to play white noise into a series of open-open pipes with varying lengths and radii for the purpose of creating standing waves within the pipe. A microphone and digital oscilloscope then recorded this data as a time-domain signal, after which a fast Fourier transform was performed on the data, converting the data into a frequency spectrum and thus displaying the resonance frequencies of the pipe as clear peaks (see Fig. 2). Fitting a model to the length, radius, and primary resonance frequency (where  $n = 1$ ) allowed us to perform a two-parameter best fit to determine the values of  $v$  and  $k$ , and subsequently compare  $v$  to literature values, within experimental uncertainties.

By fitting the end-correction resonance frequency model to the resonance frequency—found from a fast Fourier transform of the white noise time-domain signal of several pipes with varying length and radius—is it possible to determine a  $v$  (speed of sound) that agrees with literature values?

## II. METHODS

The goal of this experiment was to fit a mathematical model to a frequency spectrum dataset, generated by playing white noise through an open-open pipe, in order to determine the local speed of sound.

Part one of this experiment involved taking the time-domain signal—collected through use of a microphone placed within the pipe as well as a digital oscilloscope—and performing a fast Fourier transform on the data to convert it to a frequency spectrum. The microphone was placed in the middle of the pipe, lengthwise (the location of a pressure antinode), in order to maximize the signal collected. Furthermore, the speaker (placed 5 cm away from the mouth of the pipe,

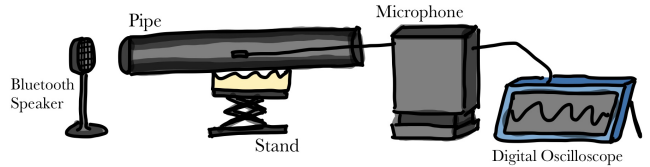


FIG. 1. Diagram illustrates the data collection setup. A bluetooth speaker is pictured at one end of the open-open pipe (shown as a cross-section), which is supported by a stand with a foam top. A microphone is shown to be inserted through the other end of the pipe and placed at the middle, lengthwise. The microphone setup is connected to the digital oscilloscope, which allows for time-domain data to be taken when sound is played through the speaker.

thereby maintaining the open-open formation of the pipe) played white noise, allowing for the collection of spectrum data from all frequencies (see Fig. 1). The collected time-domain signal was then fast Fourier transformed into frequency spectrum data using the `fft` and `fft freq` packages in Python, and best fits to the Lorentzian function were performed to determine the primary resonance frequency (see Fig. 2). These fits were performed on the first resonance frequency peak (corresponding to the lowest resonance frequency). This process was repeated for a number of pipes, each of varying length and diameter—these values were determined by ruler and caliper measurements, where the diameter of the pipe was measured based on the inner dimensions of the pipe.

The resonance frequency and uncertainty in resonance frequency of each pipe were noted down along with its length and radius (see Table I). The dominant source of uncertainty was considered to be the uncertainty in resonance frequency, given by the 68% confidence interval; length and radius uncertainties were small enough to be considered negligible. A two-parameter fit was performed using `curvefit` and the model equation  $f = \frac{nv}{2(L+kR)}$ , through which the parameters  $v$  (speed of sound) and  $k$  (end correction coefficient) were determined.

TABLE I. Length, radius, and resonance frequency for pipes used.

	<b>Length</b> <b>m</b>	<b>Radius</b> <b>m</b>	<b>Frequency</b> <b>Hz</b>
1	$0.261 \pm 0.0005$	$0.0135 \pm 0.0005$	$621.5 \pm 7.981865$
2	$0.543 \pm 0.0005$	$0.0135 \pm 0.0005$	$306.9 \pm 11.790170$
3	$0.377 \pm 0.0005$	$0.0175 \pm 0.0005$	$431.0 \pm 7.659335$
4	$0.474 \pm 0.0005$	$0.0175 \pm 0.0005$	$345.3 \pm 4.292095$
5	$0.482 \pm 0.0005$	$0.020 \pm 0.0005$	$337.7 \pm 8.141750$
6	$0.603 \pm 0.0005$	$0.020 \pm 0.0005$	$272.9 \pm 5.664900$

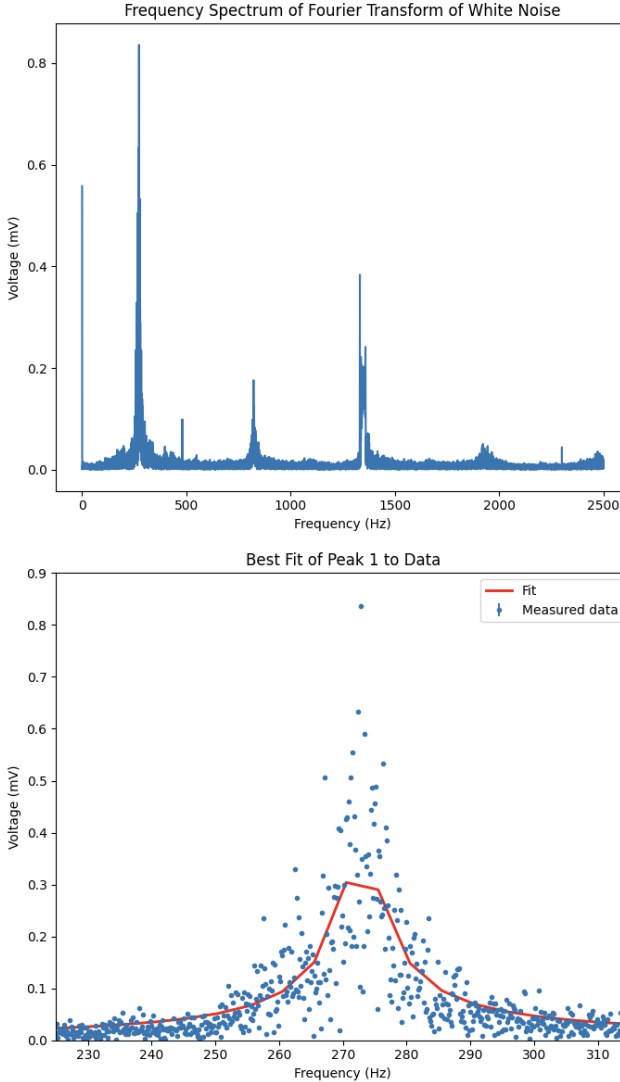


FIG. 2. The frequency spectrum of a Fourier transform of white noise, and the best fit of the first resonance frequency, for Pipe #6 (with length 0.603 m and radius 0.020 m). Error bars are too small to be seen. Outliers are shown in the frequency spectrum graph, where sudden isolated peaks arise. These can be differentiated from true resonance frequencies due to the gradual rise in voltage that appears around the resonance frequency peaks, which do not appear around the outliers. In the full frequency spectrum graph (left), four distinct peaks correspond to resonance and half-resonance frequencies, and are seen at approximately 270 Hz, 800 Hz, 1400 Hz, and 1950 Hz. Fitting the model to the resonance peak at approximately 270 Hz provides an analytically determined exact resonance frequency of  $272.9 \pm 2.917 \times 10^{-3}$  Hz.

### III. RESULTS AND DISCUSSION

The plot of length and radius to resonance frequency is shown in Fig. 3, and plots of length to resonance frequency and radius to resonance frequency are shown in Fig. 4. It can

be seen that the data followed the model quite well—the surface is a good fit for all data points—with error bars that are too small to be seen.

The two-parameter fit to the data yielded a local speed of sound of  $337.5 \pm 13.81$  m/s, and an end correction coefficient of  $1.620 \pm 1.971$ . The end correction coefficient agrees with the literature value of 1.2 [2] within uncertainties. Similarly, the speed of sound parameter matches literature values—the expected value is 343.7 m/s, which lies within the range of uncertainty.

Although the values found matched literature values within uncertainties, the uncertainties were sizeable. The end correction coefficient uncertainty was quite high in particular. The relative uncertainty in the experimentally determined speed of sound is 4%, which is not high, but higher levels of precision can still be reached.

There were a few possible contributing factors to the high uncertainties. Firstly, there was significant background noise when the experiment was carried out. This could have introduced noise in the data that would have interfered with the precise determination of the resonance frequency. Future experiments should try to mitigate this factor by reducing background noise within the lab.

Furthermore, a Lorentzian best fit was used to find the resonance frequency (see Fig. 2); although a 68% confidence interval was used for the uncertainty, there could still be some error that was unaccounted for, especially if the data was not particularly high quality (ex. low signal-to-noise ratio, outliers). However, this does not seem to be the primary source of uncertainty; it seems that the analytical resonance frequency (best fit) matches well to what is able to be visually determined from the graph, and the uncertainty in the resonance frequencies is not large (with the highest relative uncertainty being 3.8% (Pipe 2, see Table I).

A third possible source of error could be the limited number of trials, especially in regards to low variance in pipe radii. This is likely to be the main factor in the high uncertainties found, particularly in the end correction coefficient. Only six pipes were used in this experiment due to time constraints; using more pipes would yield a larger number of data points for fitting, which would consequently yield more precise parameter values. Specifically, the range of pipes used did not have a large variance in radii, and since the end correction coefficient is multiplicative with the radius in the model  $f = \frac{nv}{2(L+kR)}$ , this small range of radii likely made it more difficult for the model to determine a precise value for  $k$ . This would also explain the comparatively lower uncertainty in the determined speed of sound. Small differences in the radius across trials would not have affected the resonance frequency as much as the lengths of the pipes did. Therefore, since there was sufficient variation in the lengths of the pipes, there was a sufficient range of data points to determine a precise fit for the speed of sound. This discrepancy in the range of radii and lengths across pipes used can also be seen visually in Fig. 4.

In conclusion, this method is viable for determining an accurate speed of sound; however, steps can be taken to de-

### Radius and Length vs. Resonance Frequency

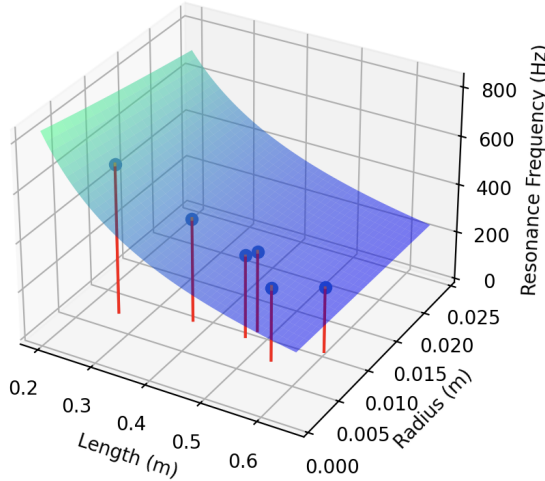


FIG. 3. A graph of length, radius, and resulting resonance frequency, plotted with the two-parameter best fit mathematical model for resonance frequency. Blue points indicate collected data, gradient surface shows the mathematical best fit, and red lines assist in visibility. Error bars are too small to be seen. The model provides a good fit to the data.

crease uncertainties and thereby increase precision.

### IV. CONCLUSION

The aim of this investigation was to determine if it was possible to experimentally find an accurate speed of sound that agreed with literature values using analytical fit methods on pipe resonance frequency data. The resonance frequencies, diameter, and length of various pipes were recorded and modelled against the formula in order to determine the variables of speed of sound and end correction factor. The results of the experiment show that it is possible to accurately determine the local speed of sound using this method; however, it requires a wider range of pipes with varying radii in order to be precise.

Using six pipes of varying length and diameter, it was found that  $k = 1.620 \pm 1.971$  and  $v = 337.5 \pm 13.81$  m/s. This study is limited in the precision of measurement. Primarily, the uncertainty in the end correction coefficient is very large. Regardless, this study effectively investigated this novel approach of determining local speed of sound, and may be useful in guiding future researchers who attempt similar experiments. Future studies in this field should repeat this ex-

periment with a larger sample size to aim at decreasing uncertainty, and complete t-score comparisons with other methods of determining the local speed of sound, such as with the use of an Arduino and ultrasonic sensor.

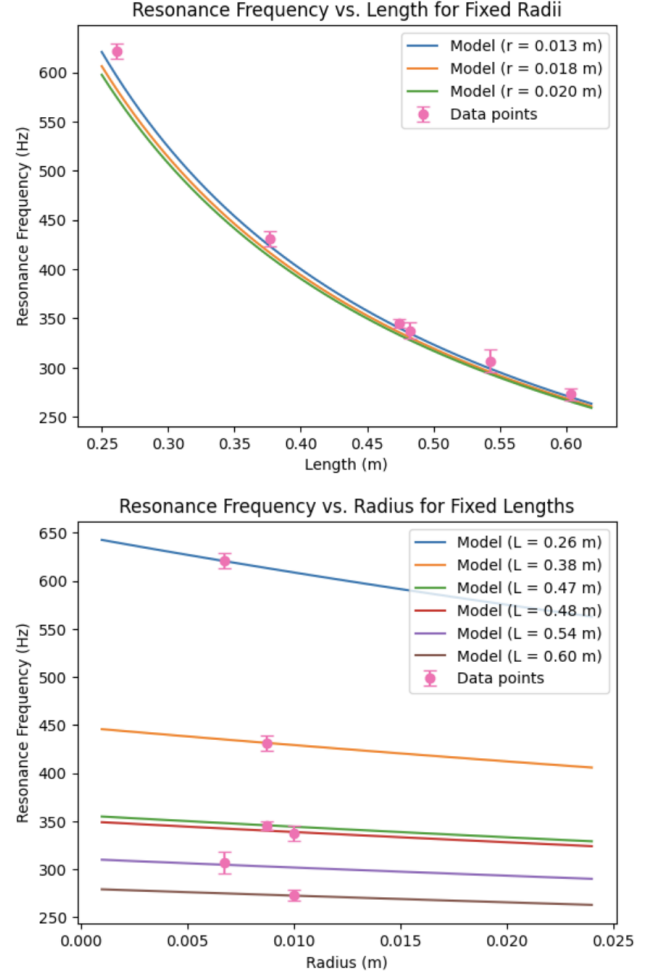


FIG. 4. A graph of length vs. resonance frequency for fixed radius values and a graph of length vs. resonance frequency for fixed length values. Data points are plotted against the two-parameter resonance frequency model. Solid lines indicate two-parameter best fit, while points with error bars show collected data. Almost all data points intersect model fits with uncertainties; the model provides a good fit to the data.

It can be important to know the local speed of sound in non-laboratory locations with varying conditions; therefore, such a method involving minimal materials and computational power can be massively useful. Thus, this novel approach to determining the local speed of sound is a promising avenue of exploration.

- 
- [1] Lab Manual - University of Tennessee. (n.d.). *Standing sound waves*. Retrieved March 24, 2025, from <http://labman.phys.utk.edu/phys221core/modules/m12/ Standing%20sound%20waves.html>
- [2] Wikipedia contributors. (November 29, 2024). *End correction*. Wikipedia. Retrieved April 6, 2025, from [https://en.wikipedia.org/wiki/End\\_correction](https://en.wikipedia.org/wiki/End_correction)